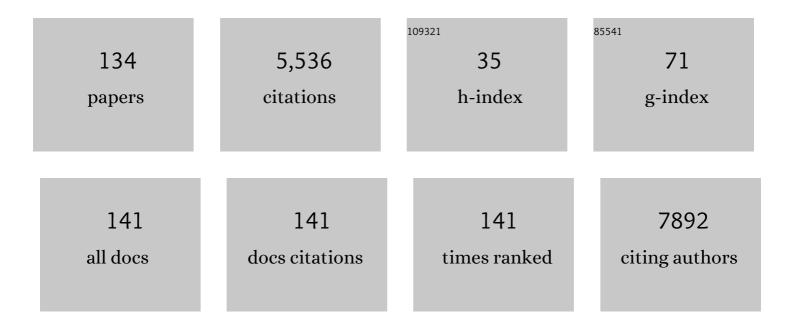
Sarah E Bohndiek

List of Publications by Year in descending order

Source: https://exaly.com/author-pdf/7358621/publications.pdf Version: 2024-02-01



SADAH F ROHNDIEK

#	Article	IF	CITATIONS
1	Opti-MSFA: a toolbox for generalized design and optimization of multispectral filter arrays. Optics Express, 2022, 30, 7591.	3.4	11
2	The Potential of Photoacoustic Imaging in Radiation Oncology. Frontiers in Oncology, 2022, 12, 803777.	2.8	11
3	Spectrally tailored 'hyperpixel' filter arrays for imaging of chemical compositions. , 2022, , .		2
4	Optimizing achromaticity in metalenses, and development of a layered thin-film metalens. , 2022, , .		0
5	Evaluation of Label-Free Confocal Raman Microspectroscopy for Monitoring Oxidative Stress In Vitro in Live Human Cancer Cells. Antioxidants, 2022, 11, 573.	5.1	5
6	SIMPA: an open-source toolkit for simulation and image processing for photonics and acoustics. Journal of Biomedical Optics, 2022, 27, .	2.6	9
7	The IPASC data format: A consensus data format for photoacoustic imaging. Photoacoustics, 2022, 26, 100339.	7.8	6
8	Photoacoustic Tomography Detects Response and Resistance to Bevacizumab in Breast Cancer Mouse Models. Cancer Research, 2022, 82, 1658-1668.	0.9	11
9	Quantification of vascular networks in photoacoustic mesoscopy. Photoacoustics, 2022, 26, 100357.	7.8	13
10	Criteria for the design of tissue-mimicking phantoms for the standardization of biophotonic instrumentation. Nature Biomedical Engineering, 2022, 6, 541-558.	22.5	20
11	DNAâ€Based Nanocarriers to Enhance the Optoacoustic Contrast of Tumors In Vivo. Advanced Healthcare Materials, 2021, 10, e2001739.	7.6	5
12	A Copolymer-in-Oil Tissue-Mimicking Material With Tuneable Acoustic and Optical Characteristics for Photoacoustic Imaging Phantoms. IEEE Transactions on Medical Imaging, 2021, 40, 3593-3603.	8.9	10
13	Multi-modal imaging of high-risk ductal carcinoma in situ of the breast using C2Am: a targeted cell death imaging agent. Breast Cancer Research, 2021, 23, 25.	5.0	3
14	Learned spectral decoloring enables photoacoustic oximetry. Scientific Reports, 2021, 11, 6565.	3.3	34
15	Spectral Endoscopy Enhances Contrast for Neoplasia in Surveillance of Barrett's Esophagus. Cancer Research, 2021, 81, 3415-3425.	0.9	14
16	Technical validation studies of a dual-wavelength LED-based photoacoustic and ultrasound imaging system. Photoacoustics, 2021, 22, 100267.	7.8	9
17	First experience in clinical application of hyperspectral endoscopy for evaluation of colonic polyps. Journal of Biophotonics, 2021, 14, e202100078.	2.3	10
18	First-in-human pilot study of snapshot multispectral endoscopy for early detection of Barrett's-related neoplasia. Journal of Biomedical Optics, 2021, 26, .	2.6	7

#	Article	IF	CITATIONS
19	Twelve tips for engaging with biologists, as told by a physicist. Nature, 2020, 577, 283-284.	27.8	1
20	A Comparative Photophysical Study of Structural Modifications of Thioflavin T-Inspired Fluorophores. Journal of Physical Chemistry Letters, 2020, 11, 8406-8416.	4.6	20
21	IPASC: a Community-Driven Consensus-Based Initiative Towards Standardisation in Photoacoustic Imaging. , 2020, , .		1
22	A background correction method to compensate illumination variation in hyperspectral imaging. PLoS ONE, 2020, 15, e0229502.	2.5	6
23	Deep learning applied to hyperspectral endoscopy for online spectral classification. Scientific Reports, 2020, 10, 3947.	3.3	37
24	ThX – a next-generation probe for the early detection of amyloid aggregates. Chemical Science, 2020, 11, 4578-4583.	7.4	43
25	Co-registration of optoacoustic tomography and magnetic resonance imaging data from murine tumour models. Photoacoustics, 2020, 18, 100147.	7.8	21
26	Photoacoustics resolves species-specific differences in hemoglobin concentration and oxygenation. Journal of Biomedical Optics, 2020, 25, .	2.6	14
27	Robustness to misalignment of low-cost, compact quantitative phase imaging architectures. OSA Continuum, 2020, 3, 2660.	1.8	1
28	A background correction method to compensate illumination variation in hyperspectral imaging. , 2020, 15, e0229502.		0
29	A background correction method to compensate illumination variation in hyperspectral imaging. , 2020, 15, e0229502.		0
30	A background correction method to compensate illumination variation in hyperspectral imaging. , 2020, 15, e0229502.		0
31	A background correction method to compensate illumination variation in hyperspectral imaging. , 2020, 15, e0229502.		0
32	A background correction method to compensate illumination variation in hyperspectral imaging. , 2020, 15, e0229502.		0
33	A background correction method to compensate illumination variation in hyperspectral imaging. , 2020, 15, e0229502.		0
34	Optoacoustic Imaging Detects Hormone-Related Physiological Changes of Breast Parenchyma. Ultraschall in Der Medizin, 2019, 40, 757-763.	1.5	8
35	Photoacoustic imaging as a tool to probe the tumour microenvironment. DMM Disease Models and Mechanisms, 2019, 12, .	2.4	57
36	Grayscale-to-Color: Scalable Fabrication of Custom Multispectral Filter Arrays. ACS Photonics, 2019, 6, 3132-3141.	6.6	65

#	Article	IF	CITATIONS
37	Coherent Imaging Through Multicore Fibres With Applications in Endoscopy. Journal of Lightwave Technology, 2019, 37, 5733-5745.	4.6	10
38	An Activatable Cancer-Targeted Hydrogen Peroxide Probe for Photoacoustic and Fluorescence Imaging. Cancer Research, 2019, 79, 5407-5417.	0.9	31
39	A clinically translatable hyperspectral endoscopy (HySE) system for imaging the gastrointestinal tract. Nature Communications, 2019, 10, 1902.	12.8	75
40	Addressing photoacoustics standards. Nature Photonics, 2019, 13, 298-298.	31.4	20
41	A roadmap for the clinical implementation of optical-imaging biomarkers. Nature Biomedical Engineering, 2019, 3, 339-353.	22.5	52
42	Characterizing Optical Fiber Transmission Matrices Using Metasurface Reflector Stacks for Lensless Imaging without Distal Access. Physical Review X, 2019, 9, .	8.9	33
43	Reconstruction of Optical Vector-Fields With Applications in Endoscopic Imaging. IEEE Transactions on Medical Imaging, 2019, 38, 955-967.	8.9	12
44	Hyperspectral imaging in biomedical applications. Journal of Optics (United Kingdom), 2019, 21, 010202.	2.2	9
45	Development of a blood oxygenation phantom for photoacoustic tomography combined with online pO2 detection and flow spectrometry. Journal of Biomedical Optics, 2019, 24, 1.	2.6	22
46	Quantitative phase and polarization imaging through an optical fiber applied to detection of early esophageal tumorigenesis. Journal of Biomedical Optics, 2019, 24, 1.	2.6	16
47	Full-field quantitative phase and polarisation-resolved imaging through an optical fibre bundle. Optics Express, 2019, 27, 23929.	3.4	14
48	Bifunctional fluorescent probes for detection of amyloid aggregates and reactive oxygen species. Royal Society Open Science, 2018, 5, 171399.	2.4	11
49	Smartâ€Dustâ€Nanorice for Enhancement of Endogenous Raman Signal, Contrast in Photoacoustic Imaging, and T2â€Shortening in Magnetic Resonance Imaging. Small, 2018, 14, e1703683.	10.0	8
50	Emerging optical methods for endoscopic surveillance of Barrett's oesophagus. The Lancet Gastroenterology and Hepatology, 2018, 3, 349-362.	8.1	15
51	Detection of early neoplasia in Barrett's esophagus using lectin-based near-infrared imaging: an ex vivo study on human tissue. Endoscopy, 2018, 50, 618-625.	1.8	21
52	Optoacoustics delineates murine breast cancer models displaying angiogenesis and vascular mimicry. British Journal of Cancer, 2018, 118, 1098-1106.	6.4	44
53	Quantitative evaluation of comb-structure correction methods for multispectral fibrescopic imaging. Scientific Reports, 2018, 8, 17801.	3.3	7
54	An active DNA-based nanoprobe for photoacoustic pH imaging. Chemical Communications, 2018, 54, 10176-10178.	4.1	6

#	Article	IF	CITATIONS
55	Oxygen-Enhanced and Dynamic Contrast-Enhanced Optoacoustic Tomography Provide Surrogate Biomarkers of Tumor Vascular Function, Hypoxia, and Necrosis. Cancer Research, 2018, 78, 5980-5991.	0.9	44
56	Raman micro-spectroscopy for accurate identification of primary human bronchial epithelial cells. Scientific Reports, 2018, 8, 12604.	3.3	51
57	Graphitic and oxidised high pressure high temperature (HPHT) nanodiamonds induce differential biological responses in breast cancer cell lines. Nanoscale, 2018, 10, 12169-12179.	5.6	17
58	Bimodal reflectance and fluorescence multispectral endoscopy based on spectrally resolving detector arrays. Journal of Biomedical Optics, 2018, 24, 1.	2.6	17
59	Application of confocal Raman micro-spectroscopy for label-free monitoring of oxidative stress in living bronchial cells. , 2018, , .		1
60	Wide-field phase imaging for the endoscopic detection of dysplasia and early-stage esophageal cancer. , 2018, , .		0
61	Evaluation of Precision in Optoacoustic Tomography for Preclinical Imaging in Living Subjects. Journal of Nuclear Medicine, 2017, 58, 807-814.	5.0	64
62	Spectral band optimization for multispectral fluorescence imaging. , 2017, , .		1
63	Quantitative imaging of tumor vasculature using multispectral optoacoustic tomography (MSOT). , 2017, , .		0
64	Evaluation of illumination systems for wide-field hyperspectral imaging in biomedical applications. , 2017, , .		1
65	Nanodiamond preparation and surface characterization for biological applications. Proceedings of SPIE, 2017, , .	0.8	2
66	Fluorescence hyperspectral imaging (fHSI) using a spectrally resolved detector array. Journal of Biophotonics, 2017, 10, 840-853.	2.3	29
67	Label-free monitoring of tissue biochemistry following traumatic brain injury using Raman spectroscopy. Analyst, The, 2017, 142, 132-139.	3.5	26
68	Assessing Oxidative Stress in Tumors by Measuring the Rate of Hyperpolarized [1-13C]Dehydroascorbic Acid Reduction Using 13C Magnetic Resonance Spectroscopy. Journal of Biological Chemistry, 2017, 292, 1737-1748.	3.4	32
69	Distance dependent photoacoustics revealed through DNA nanostructures. Nanoscale, 2017, 9, 16193-16199.	5.6	15
70	Optoacoustic Detection of Early Therapy-Induced Tumor Cell Death Using a Targeted Imaging Agent. Clinical Cancer Research, 2017, 23, 6893-6903.	7.0	25
71	Photoacoustic imaging using genetically encoded reporters: a review. Journal of Biomedical Optics, 2017, 22, 070901.	2.6	72
72	Evaluation of illumination system uniformity for wide-field biomedical hyperspectral imaging. Journal of Optics (United Kingdom), 2017, 19, 045301.	2.2	19

#	Article	IF	CITATIONS
73	Towards Quantitative Evaluation of Tissue Absorption Coefficients Using Light Fluence Correction in Optoacoustic Tomography. IEEE Transactions on Medical Imaging, 2017, 36, 322-331.	8.9	73
74	Imaging biomarker roadmap for cancer studies. Nature Reviews Clinical Oncology, 2017, 14, 169-186.	27.6	792
75	Tolerancing the alignment of large-core optical fibers, fiber bundles and light guides using a Fourier approach. Applied Optics, 2017, 56, 3303.	1.8	0
76	Oxygen Enhanced Optoacoustic Tomography (OE-OT) Reveals Vascular Dynamics in Murine Models of Prostate Cancer. Theranostics, 2017, 7, 2900-2913.	10.0	83
77	Current and Emerging Technologies for Probing Molecular Signatures of Traumatic Brain Injury. Frontiers in Neurology, 2017, 8, 450.	2.4	18
78	A multispectral endoscope based on spectrally resolved detector arrays. Proceedings of SPIE, 2017, , .	0.8	3
79	Towards a simulation framework to maximize the resolution of biomedical hyperspectral imaging. Proceedings of SPIE, 2017, , .	0.8	4
80	Abstract 2866: Volumetric optoacoustic imaging of tumor cell death using a targeted imaging agent. , 2017, , .		0
81	Measurement of changes in blood oxygenation using Multispectral Optoacoustic Tomography (MSOT) allows assessment of tumor development. , 2016, , .		1
82	Hyperspectral fluorescence imaging with multi wavelength LED excitation. Proceedings of SPIE, 2016, ,	0.8	4
83	Design and validation of a near-infrared fluorescence endoscope for detection of early esophageal malignancy. Journal of Biomedical Optics, 2016, 21, 084001.	2.6	23
84	Contrast agents for molecular photoacoustic imaging. Nature Methods, 2016, 13, 639-650.	19.0	979
85	In vivo light fluence correction for determination of tissue absorption coefficient using Multispectral Optoacoustic Tomography. , 2016, , .		0
86	Design and validation of a near-infrared fluorescence endoscope for detection of early esophageal malignancy using a targeted imaging probe. Proceedings of SPIE, 2016, , .	0.8	0
87	Abstract 4198: Optoacoustic imaging of blood vasculature and study of angiogenesis in orthotopic breast cancer models. Cancer Research, 2016, 76, 4198-4198.	0.9	1
88	Light fluence correction for quantitative determination of tissue absorption coefficient using multi-spectral optoacoustic tomography. , 2015, , .		0
89	Single-Pixel Phase-Corrected Fiber Bundle Endomicroscopy With Lensless Focussing Capability. Journal of Lightwave Technology, 2015, 33, 3419-3425.	4.6	5
90	Evaluation of multispectral optoacoustic tomography (MSOT) performance in phantoms and in vivo. , 2015, , .		1

#	Article	IF	CITATIONS
91	Experimental evaluation of a hyperspectral imager for near-infrared fluorescent contrast agent studies. Proceedings of SPIE, 2015, , .	0.8	1
92	Photoacoustic Tomography Detects Early Vessel Regression and Normalization During Ovarian Tumor Response to the Antiangiogenic Therapy Trebananib. Journal of Nuclear Medicine, 2015, 56, 1942-1947.	5.0	72
93	Light fluence correction for quantitative determination of tissue absorption coefficient using multi-spectral optoacoustic tomography. , 2015, , .		2
94	Quantitation of a spin polarizationâ€induced nuclear Overhauser effect (SPINOE) between a hyperpolarized 13 Câ€labeled cell metabolite and water protons. Contrast Media and Molecular Imaging, 2014, 9, 182-186.	0.8	13
95	Cellulose nanoparticles: photoacoustic contrast agents that biodegrade to simple sugars. Proceedings of SPIE, 2014, , .	0.8	1
96	Analysis of image heterogeneity using 2D Minkowski functionals detects tumor responses to treatment. Magnetic Resonance in Medicine, 2014, 71, 402-410.	3.0	46
97	Gold nanorods combine photoacoustic and Raman imaging for detection and treatment of ovarian cancer. , 2014, , .		1
98	Cellulose nanoparticles are a biodegradable photoacoustic contrast agent for use in living mice. Photoacoustics, 2014, 2, 119-127.	7.8	48
99	Abstract 2047: Molecular photoacoustic imaging and serum diagnostics rapidly detect response to angiopoietin 1 and 2 blockade in ovarian cancer. , 2014, , .		0
100	Molecular Photoacoustic Imaging of Follicular Thyroid Carcinoma. Clinical Cancer Research, 2013, 19, 1494-1502.	7.0	107
101	Stable phantoms for characterization of photoacoustic tomography (PAT) systems. Proceedings of SPIE, 2013, , .	0.8	1
102	A small animal Raman instrument for rapid, wide-area, spectroscopic imaging. Proceedings of the National Academy of Sciences of the United States of America, 2013, 110, 12408-12413.	7.1	185
103	The good mentorship guide. Physics World, 2013, 26, 44-45.	0.0	0
104	Development and Application of Stable Phantoms for the Evaluation of Photoacoustic Imaging Instruments. PLoS ONE, 2013, 8, e75533.	2.5	94
105	Magnetic resonance imaging with hyperpolarized [1,4- ¹³ C ₂]fumarate allows detection of early renal acute tubular necrosis. Proceedings of the National Academy of Sciences of the United States of America, 2012, 109, 13374-13379.	7.1	99
106	Hyperpolarized 13C Spectroscopy Detects Early Changes in Tumor Vasculature and Metabolism after VEGF Neutralization. Cancer Research, 2012, 72, 854-864.	0.9	73
107	Improving Image Quality by Accounting for Changes in Water Temperature during a Photoacoustic Tomography Scan. PLoS ONE, 2012, 7, e45337.	2.5	25
108	Hyperpolarized [1- ¹³ C]-Ascorbic and Dehydroascorbic Acid: Vitamin C as a Probe for Imaging Redox Status in Vivo. Journal of the American Chemical Society, 2011, 133, 11795-11801.	13.7	177

#	Article	IF	CITATIONS
109	Tumor imaging using hyperpolarized ¹³ C magnetic resonance spectroscopy. Magnetic Resonance in Medicine, 2011, 66, 505-519.	3.0	229
110	Hyperpolarized ¹³ C MRI and PET: In Vivo Tumor Biochemistry. Journal of Nuclear Medicine, 2011, 52, 1333-1336.	5.0	52
111	Magnetization transfer measurements of exchange between hyperpolarized [1- ¹³ C]pyruvate and [1- ¹³ C]lactate in a murine lymphoma. Magnetic Resonance in Medicine, 2010, 63, 872-880.	3.0	107
112	Optical characterisation of a CMOS active pixel sensor using periodic noise reduction techniques. Nuclear Instruments and Methods in Physics Research, Section A: Accelerators, Spectrometers, Detectors and Associated Equipment, 2010, 620, 549-556.	1.6	13
113	Characterisation of regional variations in a stitched CMOS active pixel sensor. Nuclear Instruments and Methods in Physics Research, Section A: Accelerators, Spectrometers, Detectors and Associated Equipment, 2010, 620, 540-548.	1.6	11
114	Detecting treatment response in a model of human breast adenocarcinoma using hyperpolarised [1-13C]pyruvate and [1,4-13C2]fumarate. British Journal of Cancer, 2010, 103, 1400-1406.	6.4	124
115	Detection of Tumor Response to a Vascular Disrupting Agent by Hyperpolarized 13C Magnetic Resonance Spectroscopy. Molecular Cancer Therapeutics, 2010, 9, 3278-3288.	4.1	66
116	Imaging and â€`omic' methods for the molecular diagnosis of cancer. Expert Review of Molecular Diagnostics, 2010, 10, 417-434.	3.1	22
117	Signal and noise transfer properties of CMOS based active pixel flat panel imager coupled to structured CsI:TI. Medical Physics, 2009, 36, 116-126.	3.0	21
118	An active pixel sensor x-ray diffraction (APXRD) system for breast cancer diagnosis. Physics in Medicine and Biology, 2009, 54, 3513-3527.	3.0	11
119	Production of hyperpolarized [1,4- ¹³ C ₂]malate from [1,4- ¹³ C ₂]fumarate is a marker of cell necrosis and treatment response in tumors. Proceedings of the National Academy of Sciences of the United States of America, 2009, 106, 19801-19806.	7.1	328
120	The Multidimensional Integrated Intelligent Imaging project (MI-3). Nuclear Instruments and Methods in Physics Research, Section A: Accelerators, Spectrometers, Detectors and Associated Equipment, 2009, 604, 196-198.	1.6	12
121	Characterization and Testing of LAS: A Prototype `Large Area Sensor' With Performance Characteristics Suitable for Medical Imaging Applications. IEEE Transactions on Nuclear Science, 2009, 56, 2938-2946.	2.0	26
122	A CMOS Image Sensor With In-Pixel ADC, Timestamp, and Sparse Readout. IEEE Sensors Journal, 2009, 9, 20-28.	4.7	16
123	A non-free-space propagation x-ray phase contrast imaging method sensitive to phase effects in two directions simultaneously. Applied Physics Letters, 2009, 94, 044108.	3.3	41
124	Comparison of Methods for Estimating the Conversion Gain of CMOS Active Pixel Sensors. IEEE Sensors Journal, 2008, 8, 1734-1744.	4.7	46
125	A CMOS active pixel sensor system for laboratory- based x-ray diffraction studies of biological tissue. Physics in Medicine and Biology, 2008, 53, 655-672.	3.0	40
126	A 54mm x 54mm — 1.8Megapixel CMOS image sensor for medical imaging. , 2008, , .		6

A 54mm x 54mm — 1.8Megapixel CMOS image sensor for medical imaging. , 2008, , . 126

8

#	Article	IF	CITATIONS
127	Development of a prototype sensor system for ultra-high-speed LDA-PIV. , 2008, , .		1
128	Correlation of energy dispersive diffraction signatures and microCT of small breast tissue samples with pathological analysis. Physics in Medicine and Biology, 2007, 52, 6151-6164.	3.0	41
129	Empirical electroâ€optical and xâ€ray performance evaluation of CMOS active pixels sensor for low dose, high resolution xâ€ray medical imaging. Medical Physics, 2007, 34, 4612-4625.	3.0	49
130	Characterization studies of two novel active pixel sensors. Optical Engineering, 2007, 46, 124003.	1.0	23
131	Optical and x-ray characterization of two novel CMOS image sensors. , 2007, , .		3
132	Characterisation of Vanilla—A novel active pixel sensor for radiation detection. Nuclear Instruments and Methods in Physics Research, Section A: Accelerators, Spectrometers, Detectors and Associated Equipment, 2007, 581, 287-290.	1.6	13
133	First evidence of phase-contrast imaging with laboratory sources and active pixel sensors. Nuclear Instruments and Methods in Physics Research, Section A: Accelerators, Spectrometers, Detectors and Associated Equipment, 2007, 581, 776-782.	1.6	19
134	Curriculum blues. Physics World, 2002, 15, 18-18.	0.0	0